



UNIVERSITY OF LEEDS

This is a repository copy of *Synthesis of the land carbon fluxes of the Amazon region between 2010 and 2020*.

White Rose Research Online URL for this paper:

<https://eprints.whiterose.ac.uk/207172/>

Version: Accepted Version

Article:

Gloor, E. orcid.org/0000-0002-9384-6341 (Accepted: 2023) Synthesis of the land carbon fluxes of the Amazon region between 2010 and 2020. Communications Earth & Environment. ISSN 2662-4435 (In Press)

This is an author produced version of an article accepted for publication in Communications Earth & Environment, made available under the terms of the Creative Commons Attribution License (CC-BY), which permits unrestricted use, distribution and reproduction in any medium, provided the original work is properly cited.

Reuse

This article is distributed under the terms of the Creative Commons Attribution (CC BY) licence. This licence allows you to distribute, remix, tweak, and build upon the work, even commercially, as long as you credit the authors for the original work. More information and the full terms of the licence here: <https://creativecommons.org/licenses/>

Takedown

If you consider content in White Rose Research Online to be in breach of UK law, please notify us by emailing eprints@whiterose.ac.uk including the URL of the record and the reason for the withdrawal request.



eprints@whiterose.ac.uk
<https://eprints.whiterose.ac.uk/>

Synthesis of the land carbon fluxes of the Amazon region between 2010 and 2020

Thais M. Rosan¹, Stephen Sitch¹, Michael O'Sullivan¹, Luana S. Basso^{2,3}, Chris Wilson^{4,5}, Camila Silva^{6,7,8}, Emanuel Gloor², Dominic Fawcett^{1,30}, Viola Heinrich¹, Jefferson G. Souza¹, Francisco Gilney Silva Bezerra³, Celso von Randow³, Lina M. Mercado^{1,9}, Luciana Gatti³, Andy Wiltshire^{1,10}, Pierre Friedlingstein¹, Julia Pongratz^{11,12}, Clemens Schwingshackl¹¹, Mathew Williams¹³, Luke Smallman¹³, Jürgen Knauer¹⁴, Vivek Arora¹⁵, Daniel Kennedy¹⁶, Hanqin Tian¹⁷, Wenping Yuan¹⁸, Atul K. Jain¹⁹, Stefanie Falk¹¹, Benjamin Poulter²⁰, Almut Arneth²¹, Qing Sun²², Sönke Zaehle²³, Anthony P. Walker²⁴, Etsushi Kato²⁵, Xu Yue²⁶, Ana Bastos²³, Philippe Ciais²⁷, Jean-Pierre Wigneron²⁸, Clement Albergel²⁹, Luiz E.O.C Aragão^{1,3}

¹Faculty of Environment, Science and Economy, University of Exeter, Exeter, UK.

²School of Geography, University of Leeds, Leeds, LS2 9JT, UK

³General Coordination of Earth Science (CGCT), National Institute for Space Research (INPE), São José dos Campos, Brazil

⁴National Centre for Earth Observation, University of Leeds, Leeds, UK

⁵School of Earth and Environment, University of Leeds, UK

⁶Instituto de Pesquisas Ambientais da Amazônia, Brasília, DF, Brazil.

⁷Lancaster Environment Centre, Lancaster University, Lancaster, UK.

⁸BeZero Carbon Ltd, London, UK.

⁹UK Centre for Ecology & Hydrology, Wallingford, OX10 8BB, UK

¹⁰Met Office Hadley Centre, UK

¹¹Department of Geography, Ludwig-Maximilians-Universität München (LMU), Munich, Germany

¹²Max Planck Institute for Meteorology, Hamburg, Germany

¹³School of GeoSciences and National Centre for Earth Observation, University of Edinburgh, Edinburgh, EH9 3FF, UK

¹⁴Hawkesbury Institute for the Environment, Western Sydney University, Penrith, NSW, Australia

¹⁵Canadian Centre for Climate Modelling and Analysis, Climate Research Division, Environment and Climate Change Canada, Victoria, BC, Canada

¹⁶National Center for Atmospheric Research, Climate and Global Dynamics,
Terrestrial Sciences Section, Boulder, CO 80305, USA

¹⁷Schiller Institute for Integrated Science and Society, Department of Earth and
Environmental Sciences, Boston College, Chestnut Hill, MA 02467, USA

¹⁸School of Atmospheric Sciences, Southern Marine Science and Engineering
Guangdong Laboratory (Zhuhai), Sun Yat-sen University, Zhuhai, 519082,
Guangdong, China

¹⁹Department of Atmospheric Sciences, University of Illinois, Urbana-Champaign, IL
61801, USA

²⁰NASA Goddard Space Flight Center, Biospheric Sciences Lab., Greenbelt, MD
20771, USA

²¹Karlsruhe Institute of Technology, Institute of Meteorology and Climate
Research/Atmospheric Environmental Research, 82467 Garmisch-Partenkirchen,
Germany

²²Climate and Environmental Physics, Physics Institute and Oeschger Centre for
Climate Change Research, University of Bern, Bern, Switzerland

²³Max Planck Institute for Biogeochemistry, P.O. Box 600164, Hans-Knöll-Str. 10,
07745 Jena, Germany

²⁴Environmental Sciences Division and Climate Change Science Institute, Oak Ridge
National Laboratory, Oak Ridge, TN, 37831, USA

²⁵Institute of Applied Energy (IAE), Minato-ku, Tokyo 105-0003, Japan

²⁶School of Environmental Science and Engineering, Nanjing University of Information
Science and Technology (NUIST), Nanjing 211544, China

²⁷Laboratoire des Sciences du Climat et de l'Environnement, LSCE/IPSL, CEA-CNRS-
UVSQ, Université Paris-Saclay, 91191 Gif-Sur-Yvette, France

²⁸ISPA, INRAE Bordeaux, 33140 Villenave d'Ornon, France

²⁹European Space Agency Climate Office, ECSAT, Harwell Campus, Didcot, UK

³⁰Swiss Federal Institute for Forest Snow and Landscape Research WSL,
Birmensdorf, Switzerland

Abstract

The Amazon is the largest continuous tropical forest in the world and plays a key
role in the global carbon cycle. Human-induced disturbances and climate change have

1 impacted the Amazon carbon balance. Here we conduct a comprehensive synthesis
2 of existing state-of-the-art estimates of the contemporary land carbon fluxes in the
3 Amazon using a set of bottom-up methods (i.e., dynamic vegetation models and
4 bookkeeping models) and a top-down inversion (atmospheric inversion model) over
5 the Brazilian Amazon and the whole Biogeographical Amazon domain. Over the whole
6 biogeographical Amazon region bottom-up methodologies suggest a small average
7 carbon sink over 2010-2020, in contrast to a small carbon source simulated by top-
8 down inversion (2010-2018). However, these estimates are not significantly different
9 from one another when accounting for their large individual uncertainties, highlighting
10 remaining knowledge gaps, and the urgent need to reduce such uncertainties.
11 Nevertheless, both methodologies agreed that the Brazilian Amazon has been a net
12 carbon source during recent climate extremes and that the south-eastern Amazon was
13 a net land carbon source over the whole study period (2010-2020). Overall, our results
14 point to increasing human-induced disturbances (deforestation and forest degradation
15 by wildfires) and reduction in the old-growth forest sink during drought.

17 **Introduction**

18 The Amazon covers an area of ~7 million km² and accounts for about 40% of
19 global tropical forest area, storing around 229-280 Pg C (Petagram of carbon) in living
20 biomass and dead organic matter in soils^{1,2}, of which approximately 108 (95% CI 101-
21 115) Pg C is aboveground in live trees³. As a result, the Amazon forest plays a key
22 role in the global carbon cycle and even small perturbations, as a consequence of
23 human disturbances⁴ and climate change, can have an impact on global climate^{5,6}, as
24 well as on South America's hydrological cycle⁷. The carbon sink contribution of the
25 old-growth forests (i.e., forests not impacted by contemporary human-induced
26 disturbances) in the Amazon has been estimated to be undergoing a persistent
27 decline, driven by an increase in tree mortality, associated with environmental
28 change⁸⁻¹¹. The old-growth Amazon forest may thus continue to lose its climate
29 change mitigation role by absorbing less carbon from the atmosphere in the future<sup>8-
30 11</sup>.

31 Alongside the effects of environmental change, in particular the increasing
32 concentration of CO₂ in the atmosphere driven by anthropogenic activities, the
33 Amazon has also been impacted by human-induced disturbances. These

disturbances are caused by large-scale land use and land cover changes (LULCC) and landscape fragmentation driven by deforestation, and extensive forest degradation through wildfires caused by anthropogenic activity in association to drier conditions and logging. These human-induced disturbances resulted in aboveground carbon (AGC) losses of 1.3 (± 0.4) Pg C between 2012 and 2019¹². After reaching the lowest deforestation rate in 2012, the Brazilian Amazon suffered an upturn with consistent intensification of deforestation rates¹³. This pattern shift in deforestation caused an increase of about 140% in CO₂ emissions in 2020 compared to the decadal low in 2012¹⁴. Moreover, the areal extent and gross carbon emissions from forest degradation can even exceed those from deforestation, especially in extreme drought years^{15–19}. Forest degradation through fire reduces the potential of secondary forests to accumulate carbon²⁰ and regrowing burned Amazon humid forests are not able to offset the initial disturbance emissions even 30 years after the fire occurrence²¹. Other processes such as logging and edge effects induced by landscape fragmentation result in additional carbon losses and subsequent carbon emissions to the atmosphere^{12,22}. When taken together, these disturbance processes increase the carbon sources impeding their offset by the carbon sink in old-growth forests, which shows evidence of a decline⁸ therefore, shifting the net carbon balance of the Amazon towards (higher) emissions to the atmosphere.

There are multiple approaches to estimate the land carbon fluxes. Bottom-up approaches comprise the use of process-based Dynamic Global Vegetation Models (DGVMs)²⁹ and bookkeeping models^{30–32}, as well as remote sensing-based estimates²⁴. Top-down approaches are based on atmospheric inversion models, which combine in situ CO₂ measurements, aircraft measurements of CO₂ concentration and atmospheric transport model simulations³³. There are discrepancies between bottom-up and top-down estimates for the South America carbon budget, with the top-down inversions estimating a net land source and bottom-up a net land sink³⁴. Studies of Amazon carbon fluxes have concentrated mostly on the roles of old-growth forests as a carbon sink⁸, on the emissions from deforestation and forest degradation^{23–25}, or on net biome productivity (NBP)^{26,27}. They use different methodologies, study periods, and spatial domains of the Amazon area (e.g., whole Amazon vs Brazilian Amazon) which causes difficulties in comparing estimates. The Brazilian Amazon forests was estimated to be a net carbon source of +0.06 (-0.01 to +0.31) Pg C yr⁻¹ in 2010 based on a literature review and compilation of datasets²⁷.

Estimates based on Earth observation data focusing on the carbon gains and losses in forest areas derived from the Global Forest change product²⁸ and using emissions and removal factors from the Intergovernmental Panel on Climate Change (IPCC) guidelines, indicated that the whole Amazon Forest region was a net carbon sink between 2001 and 2019, while the Brazilian part of the Amazon forest acted as a net carbon source as a result of deforestation²⁴. A study using in situ observations of gases (e.g., CO and CO₂) by aircraft-borne flasks and an atmospheric transport inverse modelling approach concluded that the Amazon region was a small net carbon source over the 2010-2018 period, driven mostly by fire emissions from the south-east Amazon region²⁶.

Knowledge gaps remain about the processes included in bottom-up models (e.g., anthropogenic wildfires and fire and drought induced tree mortality^{21,35}), the land use and land cover change data used in these model simulations³⁶, as well as consistent uncertainty estimates. Therefore, a synthesis and standardisation of existing estimates of the net land carbon fluxes of the Amazon region is needed to characterize the contemporary state of the net land carbon fluxes, and to clarify where the main gaps remain to reconcile differences of flux estimates between top-down and bottom-up approaches. Given the importance of the Amazon for the global carbon cycle and the recent changes in deforestation pattern, the main aim of this study is to provide a comprehensive state-of-the-art synthesis of the net land-atmosphere carbon flux of the whole Amazon as well as the Brazilian Amazon area for the 2010-2020 period.

Here we quantify the net land carbon fluxes of the whole biogeographical domain of the Amazon³⁷ and of the Brazilian Amazon, using existing data from top-down atmospheric transport inversion³⁸, and a combination of bottom-up model-based estimates^{23,32,39}. To estimate the net carbon sources from human-induced forest disturbances, we use a set of bottom-up estimates of disturbance fluxes including deforestation and forest degradation and subsequent regrowth using regional^{23,32} and global spatially explicit bookkeeping models^{31,39,40}. These bookkeeping models are constrained with satellite estimates of deforestation and degradation area and use response curves of decomposition and tree growth to estimate the resulting net carbon fluxes caused by deforestation and degradation (see further detail of each model in the Methods section). To estimate the net carbon sink of old-growth forests, we use a set of Dynamic Global Vegetation Models (DGVMs) which participated in the Global Carbon Budget 2022 (GCB)³⁹ assessment, called TRENDY-v11. We then combine all

estimates of net sources and sinks from the bottom-up models to calculate the spatiotemporal net land carbon fluxes for the whole Biogeographical Amazon and for the Brazilian Amazon, separately (see domain limits in SI Figure 1 and model combinations in Table 3 of Methods section). Finally, we synthesize and present the net land carbon fluxes based on the bookkeeping models combination with TRENDY-v11 DGVMs (bottom-up estimates), the bottom-up net flux estimate from the CARDAMOM model-data fusion framework^{41,42} and top-down atmospheric inversion estimates (TOMCAT) using a global atmospheric transport model³⁸ that is constrained with atmospheric profile measurements²⁶. Figure 1 shows an overview of the methodologies used to estimate the carbon fluxes of each domain. Note that the model combination used to calculate the net land carbon fluxes with bookkeeping models and TRENDY-v11 DGVMs differs between the whole Biogeographical Amazon and Brazilian Amazon due to differences in data availability for each region as described in Table 3 in the methods section. Hereafter we adopt a + sign convention to represent a net flux of carbon from land to the atmosphere (source) and a - sign convention for a net carbon flux into the land (sink).

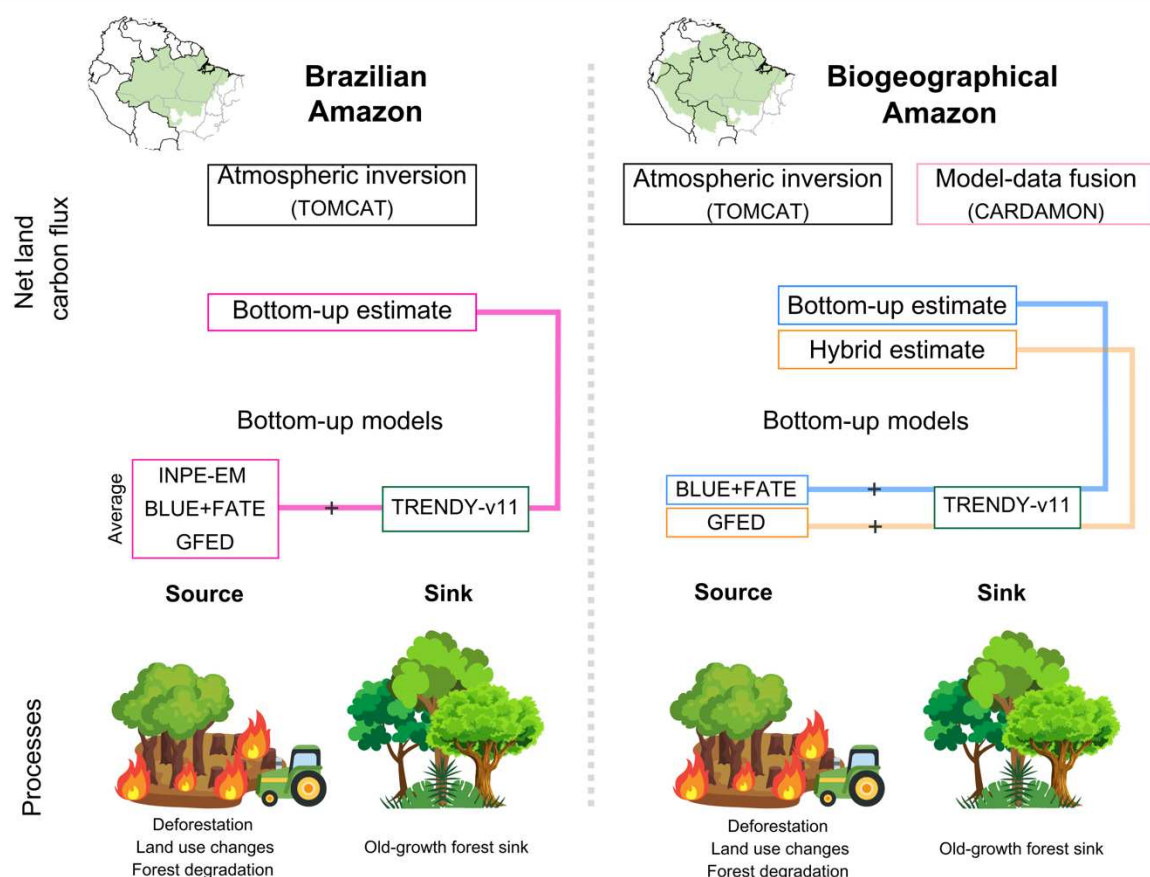


Figure 1 Overview of the existing methodologies applied to estimate the carbon

fluxes in the Brazilian Amazon and Biogeographical Amazon according to data availability. Details of each bookkeeping models (INPE-EM, BLUE, FATE and GFED), TRENDY-v11 DGVMs, TOMCAT atmospheric inversion (called top-down inversion in the results section) and CARDAMON can be found in the methods section and their combinations in Table 3. Further detailed information about the processes included in each model can be found in Table 2 and SI Table 3 for the TRENDY-v11 DGVMs.

Results

Spatiotemporal attribution of the land carbon fluxes in the whole biogeographical Amazon

For the whole biogeographical Amazon, we relied on two global models to estimate the disturbance flux. A combination of net land use flux estimates from the Bookkeeping of Land Use Emissions (BLUE) added to the net wildfire flux from a fire bookkeeping model (FATE) (BLUE+FATE, see Methods), suggests the whole biogeographical Amazon released a net flux of 192 Tg C yr⁻¹ over 2010-2020 to the atmosphere from land use and land cover changes and forest degradation fires. Over the same period, the Global Fire Emissions Database (GFED) suggested an average flux of 89 Tg C yr⁻¹ from deforestation and degradation fires (Table 1). Both BLUE+FATE and GFED show similar interannual variability (Figure 2a). However, the average flux simulated by BLUE+FATE is 116% higher than GFED, as the former includes more processes linked to land use and land cover changes, such as fluxes from transitions between different land uses, shifting cultivation, soil carbon and legacy fluxes, as well as the addition of the net legacy fluxes of forest degradation by fire from the FATE model, which include late tree mortality by fire. The GFED estimates used here only account for biomass burning flux from tropical forest fires linked to deforestation and degradation but assume that degraded forests are carbon neutral (i.e., GFED does not include late tree mortality fluxes). Spatially, both models show that most of the net disturbance fluxes are concentrated in the south-eastern Amazon region (i.e., in the Southern Brazilian Amazon) (Figure 2c-2d). As none of the two models used to estimate the disturbance flux for the whole Biogeographical Amazon provides regional uncertainty estimates, we are unable to quantify the uncertainty for the disturbance term.

The average old-growth forest sink simulated by TRENDY-v11 DGVMs (16 models) for the whole biogeographical Amazon was $-333 (\pm 195)$ Tg C yr⁻¹ over the 2010-2020 period (Table 1). The old-growth forest sink shows a high interannual variability driven by intense drought events which causes a water stress in the vegetation⁴³ and is associated to the El Niño–Southern Oscillation (ENSO) years over our study period ($R = -0.6$; $p = 0.051$ in SI Figure 2c). Those drought events reduce the sink capacity of these forests in our estimates due to the reduced simulated productivity in the DGVMs (e.g., 2015/2016 in Figure 2b). Spatially, the average old-growth forest sink was higher in the western and northern parts of the Amazon (Figure 2e) where most of the old-growth forest is located. Lower values occur across the south-eastern regions along the areas with lower intact old-growth forest percentage due to deforestation and degradation (see the fraction mask of old-growth forests applied to the DGVMs in SI Figure 5). Stronger patterns in the old-growth forest sink, such as the pink grid-cells in Figure 2e, are driven by lower annual precipitation (<1000 mm) during the 2015/2016 ENSO in the precipitation data used as input in the TRENDY-v11 DGVMs (SI Figure 3). Several DGVMs simulate a stronger transition of the old-growth forest from sink to source in this region in 2015/2016, which dominates the decadal mean flux (SI Figure 4). This localized pattern points to the general sparsity of climate datasets across this important region for interpolation in reanalysis datasets, which are used as input for the DGVMs simulations.

Between 2010 and 2015 the old-growth forest sink based on field data from the Amazon Forest Inventory Network (RAINFOR) upscaled to the Amazon was -271 (CI $0.00-502$) Tg C yr⁻¹^{9,44}. The old-growth forest sink simulated by TRENDY-v11 DGVMs was 26% larger than RAINFOR over the same period (average of -348 ± 167 Tg C yr⁻¹). Although there is a difference in magnitude between the TRENDY DGVMs and the RAINFOR intact sink, they are not statistically significantly different over this period ($p = 0.37$; SI Figure 8). We also compared the aboveground carbon (AGC) change in intact areas between the TRENDY-v11 multi-model mean and AGC derived from satellite data from the L-Band Vegetation Optical Depth (L-VOD) from a recent study¹². Although L-VOD based AGC shows an average net loss of carbon to the atmosphere of about 35 Tg C yr⁻¹ and TRENDY-v11 AGC an average net carbon gain to the land of 26 Tg C yr⁻¹ over the period of 2011-2019, a Welch's t-test shows that their average values over this common period is not significantly different ($p = 0.5$; SI Figure 9). Note

that these values need to be compared cautiously due to potential differences in their old-growth forest mask and Amazon area, as well as in the processes included.

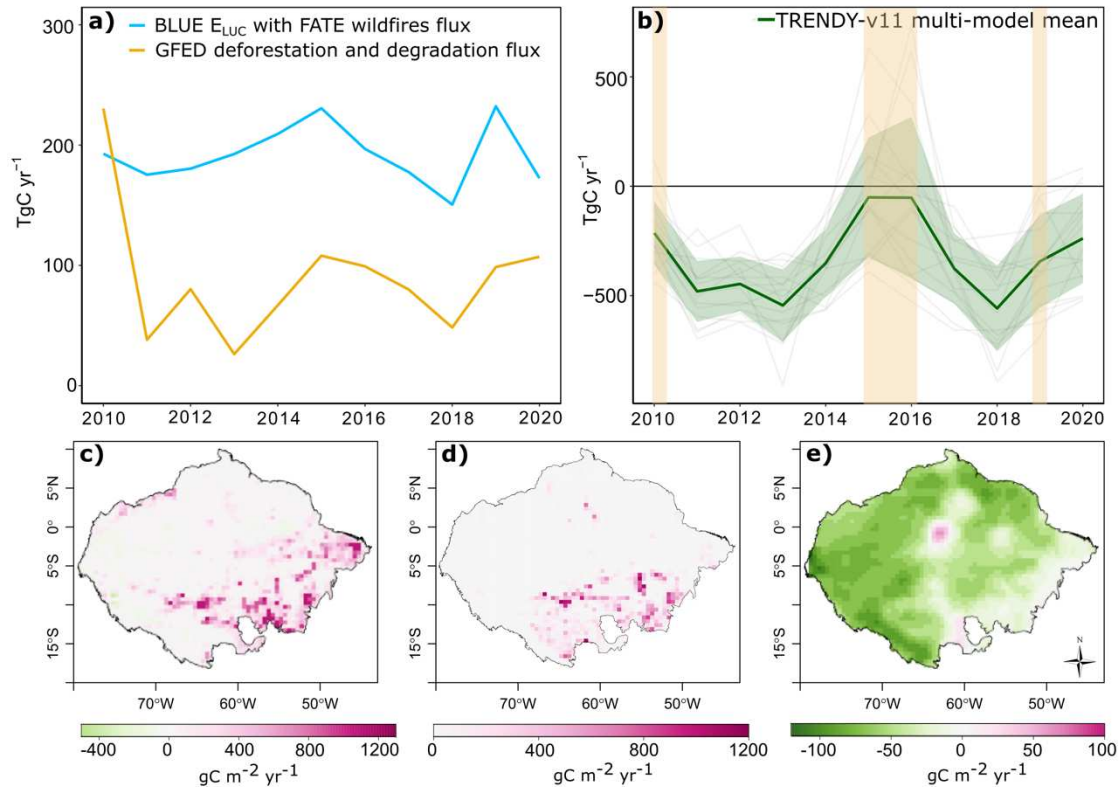


Figure 2 Attribution of the land carbon fluxes in the biogeographical Amazon over 2010-2020 from bottom-up and hybrid model combinations. A) Annual net disturbance fluxes from BLUE land use and land cover changes (BLUE E_{LUC}) with FATE forest degradation fires, and GFED deforestation and degradation fires; **b)** Annual old-growth forest sink from TRENDY-v11 S2 simulations; shaded green area represents 1SD of the multi-model average and shaded orange area represents the ENSO years, which cause strong drought events and consequent water stress in the Amazon forests, and therefore a transition from sink to source in the old-growth forests ($R = -0.6$, $p = 0.051$; see SI Figure 2c for a correlation between the old-growth sink annual variation and a drought index); **c)** Mean annual land use and land cover flux from BLUE with wildfire flux from FATE ($\text{gC m}^{-2} \text{yr}^{-1}$), negative values in this map show a sink from land use abandonment, secondary forest regrowth and/or regrowth after harvest; **d)** Mean annual deforestation and degradation fires from GFED ($\text{gC m}^{-2} \text{yr}^{-1}$); **e)** Mean annual old-growth forest sink from TRENDY-v11 ($\text{gC m}^{-2} \text{yr}^{-1}$). The spatial uncertainty from the TRENDY-v11 old-growth sink is shown in SI Figure 10. Positive

values (in pink) indicate sources to the atmosphere and negative values (in green) indicate sinks.

Spatiotemporal attribution of the land carbon fluxes in the Brazilian Amazon

A three-model combination that provides the net fluxes of forest disturbances (deforestation + degradation, including regrowth of these processes) was used to calculate one average estimate of the net disturbance flux (see Table 3 in Methods). We combine these three anthropogenic disturbances estimates due to the availability of regional estimates based on the official deforestation data from the Brazilian Amazon Monitoring Program (PRODES), as well as to be able to provide an estimate of the spread (uncertainty) for the Brazilian Amazon anthropogenic disturbance fluxes. The results show that the Brazilian Amazon released an average net flux of 115 Tg C yr⁻¹ (± 68 ; 1SD multi-model range) to the atmosphere from all forest disturbances between 2010 and 2020 (Figure 3a, black line). The multi-model mean net disturbance flux (Figure 3a, black line) shows emission peaks in 2010, 2015 and an increased flux after 2018. The differences in the magnitude of individual disturbance models used to calculate the average disturbance flux for the Brazilian Amazon is due to the processes included and different driving data (see Methods section and Table 3 for further details of the main processes included in each model). Spatially, the disturbance fluxes are concentrated in the 'arc of deforestation' region in the southern Brazilian Amazon and along major roads that facilitate the advance of deforestation and spread of fires into forest edges (Figure 3c).

Annual estimates of old-growth forest cover loss from the Brazilian Amazon Monitoring Program of the Instituto Nacional de Pesquisas Espaciais (PRODES/INPE) show that 2020 had the highest deforestation area in old-growth forest in the last decade¹³. This large area of deforestation in 2020 led to an increase of 12% (from 68 Tg C to 76 Tg C) in the emissions estimated by the INPE emission model (INPE-EM) compared to 2019⁴⁵. Yet, the multi-model disturbance average (black line in Figure 3a) did not reproduce higher emissions in 2020 compared to 2019, which is due to the BLUE and GFED models showing a decrease in emissions between these two years (blue and orange lines in Figure 3a). The reason for the diverging results between INPE-EM and the other two models is because they use different driving data and mapping calendar (see Methods for detailed information). The INPE-EM uses the

1 Brazilian official deforestation dataset (PRODES/INPE) as driving data of the
2 deforestation area. The area estimates are calculated based on observations from
3 satellite data (e.g., Landsat) between August and July (e.g., August 2019 – July 2020).
4 Moreover, PRODES/INPE only track deforestation within their old-growth forest mask.
5 The BLUE model uses as the Global Land Use Harmonization database (LUH2) to
6 estimate the area impacted by land use changes, which rely on changes in agricultural
7 areas to model the deforested area within old-growth and secondary forests in a
8 calendar year (January-December). The GFED data used here is based on burned
9 areas estimates associated to deforestation and degradation in tropical forests
10 estimated from satellite data (MCD64 A1 product⁴⁶) in a calendar year (January-
11 December). Therefore, the different map periods in addition to the different methods
12 to calculate the forest area loss, as well as the processes included are likely the
13 reasons of the differences between the INPE estimates and the two other models
14 based on global products.

15 In old-growth forests, the simulated sink by the TRENDY-v11 DGVMs for the
16 Brazilian Amazon was $-170 (\pm 144) \text{ Tg C yr}^{-1}$ between 2010 and 2020. This is about
17 51% of the old-growth sink simulated for the whole Amazon in this study (-333 ± 195
18 Tg C yr^{-1}). Most of the simulated old-growth forests sink is concentrated in the central-
19 western part of the Brazilian Amazon (Figure 3d), where most of the old-growth forests
20 are located. Likewise, as was explained in the Biogeographical Amazon section, the
21 strong pink pattern in the old-growth forest sink (Figure 3d) is driven by lower annual
22 precipitation during the 2015/2016 ENSO (SI Figure 3) and the simulated response
23 from DGVMs to this lower precipitation in the decadal mean flux (SI Figure 4).

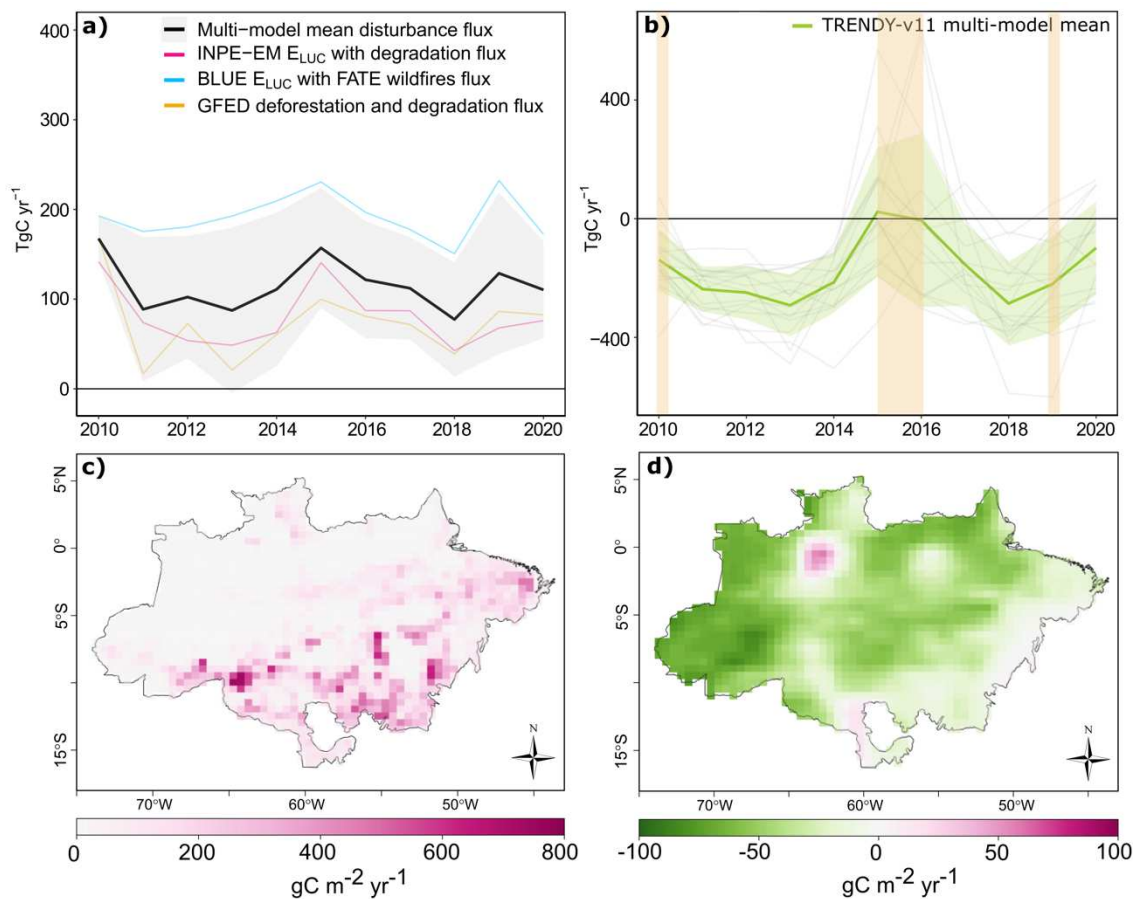


Figure 3 Attribution of the land carbon fluxes in the Brazilian Amazon over 2010-2020 from bottom-up models. **a)** Annual net disturbance fluxes from the disturbance multi-model average (see Table 2-3 in Methods section); shaded grey area represents the 1SD of the multi-model average; individual uncertainty is not available for each model; **b)** Annual old-growth land sink from TRENDY-v11 S2 simulations; shaded green area represents the 1SD of the TRENDY-v11 DGVMs mean and shaded orange areas represent the ENSO years, which cause stronger drought events in the Amazon and consequent water stress and therefore a reduction in the old-growth sink ($R = -0.88$, $p < 0.001$; see SI Figure 2b for a correlation between the old-growth sink annual variation and a drought index); **c)** Multi-model mean annual disturbance flux ($\text{gC m}^{-2} \text{yr}^{-1}$); **d)** Multi-model mean annual old-growth land sink from TRENDY-v11 S2 simulation ($\text{gC m}^{-2} \text{yr}^{-1}$). The spatial uncertainty of c and d can be found in SI Figure 7. Positive values (pink) indicate a net carbon source to the atmosphere and negative values (green) indicate a net sink.

Net land carbon flux in the whole biogeographical Amazon

Over the whole biogeographical Amazon, results of the net land carbon flux estimate from the bottom-up, hybrid and data assimilation (e.g., CARDAMOM) approaches suggest that the region was a net land carbon sink of $-152(\pm 192)$ Tg C yr⁻¹, $-255(\pm 192)$ Tg C yr⁻¹ and -339 (CI $-2945 - 2452$) Tg C yr⁻¹ between 2010 and 2018, respectively (Figure 4a and Table 1). The top-down inversion suggests a small net land carbon source of $+27 (\pm 130)$ Tg C yr⁻¹ (2010-2018) (Figure 4a and Table 1). During the drought years of 2010 and 2015/2016, the bottom-up, hybrid, and top-down inversion approaches agree that the whole Amazon was a small net carbon source while CARDAMOM suggests it was carbon neutral. Over 2019 and 2020, the bottom-up, hybrid, and CARDAMOM estimates suggest the whole biogeographical Amazon to be a net land carbon sink (Table 1). However, large uncertainties remain in all estimates. Spatially, all the models show that the south-eastern Amazon (Figure 4b-c and SI Figures 14b,15a) was a carbon source to the atmosphere driven by land use and land cover changes, forest degradation and the effects of intense drought events such as the strong 2015/2016 El Niño.

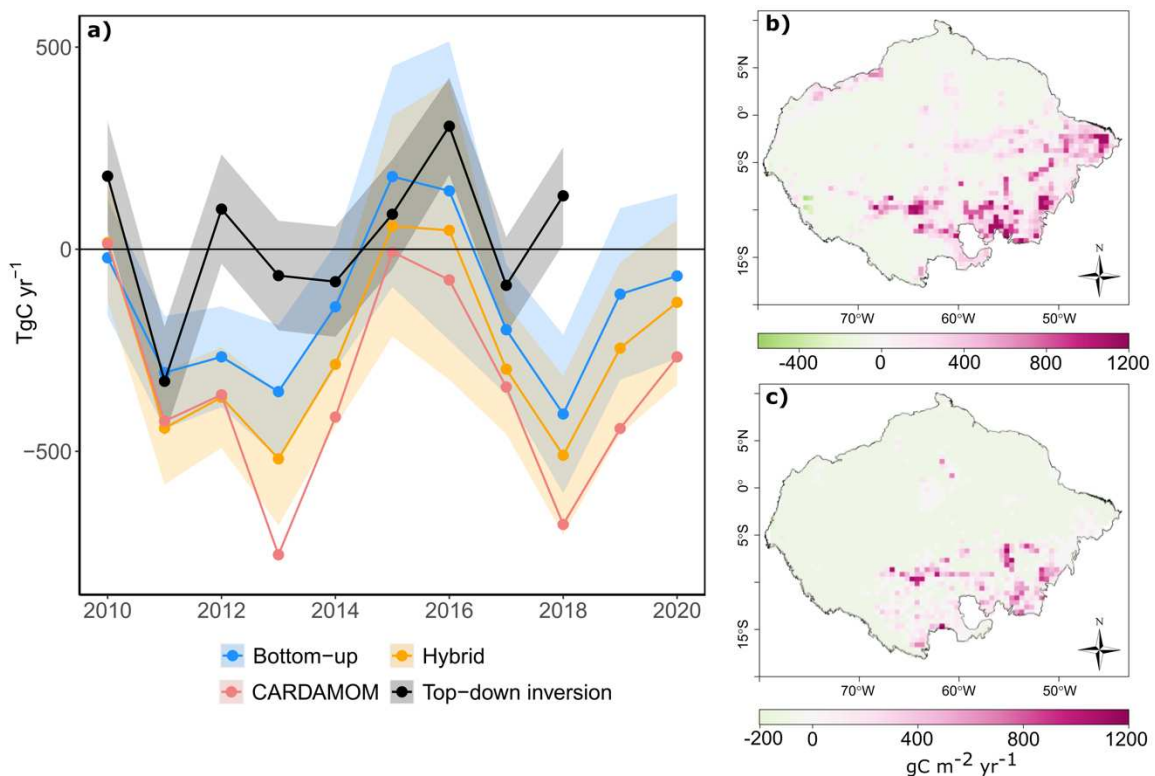


Figure 4 The net land carbon fluxes in the biogeographical Amazon. a) Annual net land carbon fluxes from the two bottom-up approaches using the anthropogenic disturbance estimates from BLUE land use and land use changes and forestry added

to FATE wildfire flux estimate (Bottom-up) and GFED deforestation and degradation fluxes (Hybrid), both added to the TRENDY-v11 intact land sink to yield the net land carbon flux; the net land carbon flux from CARDAMOM model and top-down atmospheric inversion; **b)** Spatiotemporal average of the net land carbon flux from the bottom-up approach (2010-2020) using the disturbances from BLUE land use and land cover changes emissions with FATE wildfire flux and TRENDY-v11 intact sink ($\text{gC m}^{-2} \text{yr}^{-1}$); **c)** Spatiotemporal average of the net land carbon flux from the Hybrid approach (2010-2020) using the GFED deforestation and degradation fluxes and TRENDY-v11 intact sink ($\text{gC m}^{-2} \text{yr}^{-1}$). The CARDAMOM uncertainty and spatial net average flux (2010-2020) can be found in SI Figure 14. The top-down spatial average net flux and its uncertainty can be found in SI Figure 15. Spatial uncertainty associated with the TRENDY-v11 old-growth forest sink over 2010-2020 can be found in SI Figure 10, both BLUE and GFED do not provide regional uncertainties. Positive values are source to the atmosphere and negative sink.

Net land carbon flux in the Brazilian Amazon

For the Brazilian Amazon, we combined the disturbance flux from the multi-model average (Figure 3a, black line) with the simulated sink in old-growth forests (Figure 3b, dark green line) to provide a bottom-up estimate of the net land carbon flux alongside the top-down inversion (see Methods for detailed information). The results from the bottom-up approach suggest that the Brazilian Amazon was a small net land carbon sink of $-59 (\pm 160) \text{ Tg C yr}^{-1}$ over the 2010-2018 period (Figure 5a and Table 1). Conversely, the top-down inversion suggests the same region as a small net carbon source of $+36 (\pm 125) \text{ Tg C yr}^{-1}$ over 2010-2018. However, given the large uncertainties in both approaches, their mean estimate over 2010-2018 is not statistically significantly different (Welch's t-test $p = 0.13$; SI Figure 11). Both approaches agree that the Brazilian Amazon was a net carbon source during the drought events of 2010 and 2015/2016. Spatially, the bottom-up approach (Figure 5b) and the top-down inversion (SI Figure 15a) agree that the south-eastern Brazilian Amazon was a net carbon source over the period of 2010-2020. Estimates from the bottom-up approach show that the Brazilian Amazon transitioned from a net land carbon sink of $-91 (\pm 186) \text{ Tg C yr}^{-1}$ in 2019 to a small net land carbon source in 2020

of +12 (± 165) Tg C yr⁻¹, driven by a decrease in the simulated old-growth forest sink by TRENDY-v11 DGVMs and in addition to large disturbance fluxes (Table 1).

There are some differences between the bottom-up and top-down inversion estimates of the net land carbon flux. The most evident difference is the opposing sign of the net land carbon flux in 2012 and 2018 between top-down and bottom-up/hybrid models. This difference is present in all model estimates over both the whole Amazon (Figure 3a) and Brazilian Amazon (Figure 5a). The top-down inversion suggests a net carbon source in 2018, which is hypothesised to be related to reduced carbon uptake in the south-eastern Amazon²⁶. Our bottom-up attribution shows a net lower disturbance flux in 2018 compared to 2015-2017 and a larger sink from old-growth forests (i.e., uptake), thus suggesting a net land carbon sink in 2018. We hypothesize that the large flux from the top-down inversion can be partly attributed to the difference in the spatial resolution of the datasets. For instance, the atmospheric inversion has a spatial resolution of 5.6°, therefore it could be potentially accounting for surrounding fluxes within these large grid-cells, such as fluxes from savanna fires and additional fluxes coming from fossil fuel emissions; these large fluxes are mostly from locations in the south and east Amazon (see 2012 and 2018 maps in SI Figure 12). The models used to estimate the net land carbon flux using the bottom-up approach have a spatial resolution that ranges from 30m to 1° (~100km) and are then expected to better constrain regional/local fluxes than the coarse spatial resolution of the top-down inversion. However, the bottom-up approach used to estimate the net land carbon flux in this study needs to be considered as a conservative estimate (i.e., potentially underestimating) the extent and magnitude of the disturbance flux due to difficulties in mapping understory fires as well as by not including additional fluxes associated with edge effects, for example, and limitations to represent the long-term impact of tree mortality on the carbon sink of old-growth forests from DGVMs. Thus, the top-down inversion could be capturing fluxes that are missing in the bottom-up approach, which could also contribute to explain the differences in specific years as well as in the magnitude and sign of the net land carbon fluxes.

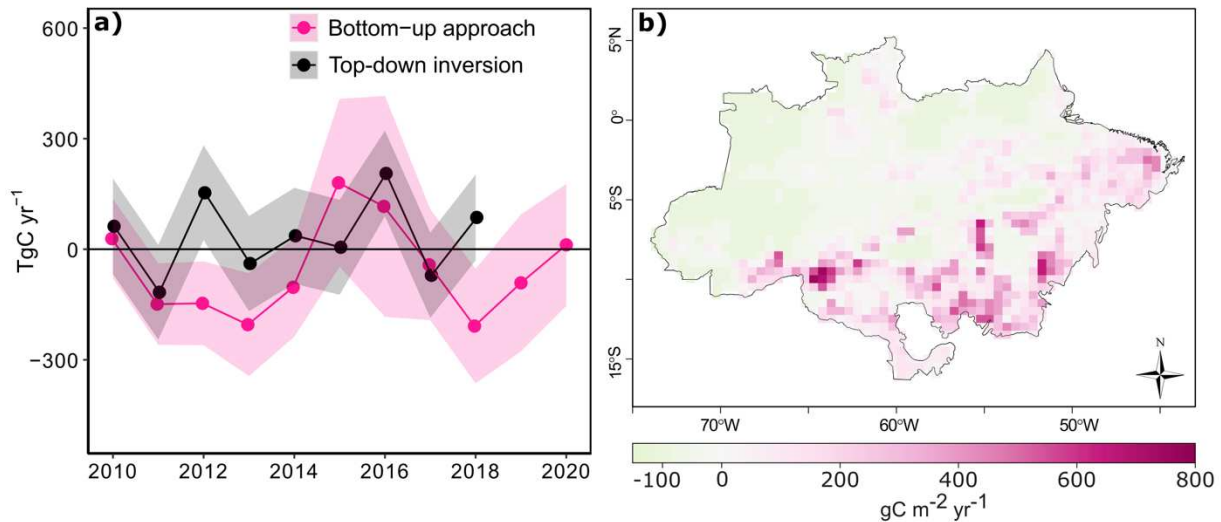


Figure 5 The net land carbon fluxes in the Brazilian Amazon. **a)** Annual net land carbon fluxes from the bottom-up approach using the combination of the multi-model mean net anthropogenic disturbance flux and TRENDY-v11 old-growth sink and top-down atmospheric inversion; shaded area represents the propagated error of both approaches (see methods); **b)** Spatial explicit bottom-up net land carbon flux over 2010-2020 ($\text{gC m}^{-2} \text{yr}^{-1}$). The spatial uncertainty over 2010-2020 can be found in SI Figure 13. Positive values are sources to the atmosphere and negative values are sinks.

Table 1 Summary table with the average ($\text{Tg C yr}^{-1} \pm 1\text{SD}$) carbon fluxes within the Brazilian Amazon and biogeographical Amazon over a common period (2010-2018). Estimates for 2019, 2020 and the average over 2010-2020 are provided separately subject to the availability of data. Individual disturbance models do not provide regional uncertainty estimates for the biogeographical Amazon. Therefore, the net land carbon flux uncertainty for the whole biogeographical Amazon is based only on the TRENDY-v11 old-growth sink uncertainty. Uncertainty estimates for CARDAMOM are provided as 95% confidence interval (CI). Further details about the single models and approaches can be found in the methods section (Table 3). The net land carbon fluxes are highlighted in bold. The annual carbon fluxes from each model used in this research (disturbances, old-growth sink and net flux) for the Brazilian Amazon and whole Biogeographical Amazon are available in the Supplementary excel tables 4 and 5, respectively.

Brazilian Amazon				
	2010-2018	2019	2020	2010-2020
Disturbances bottom-up (Multi-model average)	+114 (± 67)	+129 (± 90)	+110 (± 54)	+115 (± 68)

Old-growth forest sink (TRENDY-v11)	-173 (± 141)	-219 (± 163)	-99 (± 156)	-170 (± 144)
Net land carbon fluxes (Bottom-up)	-59 (± 160)	-91 (± 186)	+12 (± 165)	-55 (163)
Net land carbon fluxes (Top-down inversion)	36 (± 125)	-	-	-
Biogeographical Amazon				
	2010-2018	2019	2020	2010-2020
Disturbances bottom-up (BLUE E _{LUC} + FATE degradation fires)	+190	+221	+161	+192
Disturbances hybrid (GFED deforestation and degradation fires)	+86	+99	+107	+89
Old-growth forest sink (TRENDY-v11)	-342 (± 192)	-343 (± 212)	-239 (± 204)	-333 (± 195)
Net land carbon fluxes (Bottom-up)	-152 (± 192)	-111 (± 212)	-66 (± 204)	-141 (± 195)
Net land carbon fluxes (Hybrid)	-255 (± 192)	-245 (± 212)	-131 (± 204)	-243 (± 195)
Net land carbon fluxes (CARDAMOM)	-339	-444	-266	-342
	(CI -2945 – 2452)	(CI -2621 – 1587)	(CI -2366 – 1666)	(CI -2863 – 2287)
Net land carbon fluxes (Top-down inversion)	+27 (± 130)	-	-	-

Discussion

Our total net disturbance flux estimates by bottom-up models suggests an average offset of about 68% and between 27%-58% of the old-growth forest carbon sink of Brazilian Amazon and biogeographical Amazon, respectively, between 2010 and 2020. Net forest disturbance emissions are large in 2010 and 2015, which is likely related to increases in wildfires in the Amazon as an outcome of anthropogenic activities in combination with intense drought⁴⁷. The increase in the net disturbance emissions after 2018 is associated with an escalation in fire activity related to recent increases in deforestation rates^{48,49}. This recent change in deforestation pattern, mostly in the Brazilian Amazon, is in response to a combination of changes in the Brazilian Forest Code in 2012, recent weakening of the Ministry of the Environment's deforestation enforcement actions, and laws that may facilitate the regularization of illegally grabbed public lands^{50,51}. If this current pattern of deforestation remains, it will likely contribute to further offsetting the old-growth forest carbon sink.

However, high uncertainties remain on the magnitude of the net disturbance fluxes, as well as the old-growth forest sink and its impacts on the Amazon carbon balance. Previous studies have shown that the bookkeeping models used in earlier Global Carbon Budget assessments were not able to capture the magnitude and trend of land use changes for the Amazon in recent years due to deficiencies in the input data^{36,52}. Major improvements were achieved by incorporating further satellite Earth Observation (EO) data for Brazil into the land use change data that are used as input in the BLUE model simulations for the Global Carbon Budget 2022³⁹, which we employ here.

We also used estimates of a fire bookkeeping model (FATE) that quantifies the long-term net carbon fluxes of burned forests in the Amazon based on inventory data from burned forests and upscales them to the Brazilian Amazon using burned area maps. Yet, this is a conservative estimate (i.e., likely an underestimate) linked to limitations of mapping the extent of burned forests in the Amazon. Uncertainties are caused by 1) difficulties in mapping low intensity understory fires; 2) limited temporal availability of Landsat images used in FATE (i.e., the satellite passes over the same region twice per month, but since the Amazon has high cloud cover it limits the number of images available for classification)⁵³. With the increasing availability of medium to high spatial resolution satellite images, such as the Sentinels from the Copernicus program, as well as higher temporal availability by integrating a range of images of different satellites, this limitation might be overcome in the future. Further work is needed to expand the wildfire emission estimates to the whole biogeographical Amazon using a set of aboveground biomass data and burned area products. This would allow a sensitivity analysis using different input data to better quantify the uncertainties related to the long-term effect of forest degradation through fire on the carbon balance.

Edge effects caused by fragmentation can induce indirect carbon losses, which were estimated to have caused gross emissions of 63 Tg C yr⁻¹ for 2001-2015²². This individual flux is unquantified in this research and should be included in future land carbon flux assessments. However, we do partially account for edge effects due to overlap of wildfires in forest edge areas, which is estimated to be around 25% of the total burned forest area¹⁹. The inclusion of additional edge effects would be possible by standardizing the same input dataset for the bottom-up models, such that we could overlay the edge and burned forest areas and separate each flux correctly. Moreover, currently there are still knowledge gaps on forest edge dynamics to produce estimates of its net carbon flux combined with wildfires on the Amazon carbon balance¹⁹. For example, the few models that consider edge-effects only include gross carbon fluxes and not the potential partial recovery. Therefore, the total disturbance flux estimate from this work can be considered conservative.

Additionally, large uncertainties remain about the contemporary trends and magnitude of the old-growth Amazon forest sink. Observations show a weakening of the Amazon Forest sink⁹. Yet, the TRENDY-v11 multi-model mean shows no significant trend in the old-growth forest sink in the last 30 years⁵⁴ (SI Figure 16). The

1 large flux and no significant decline in the old-growth forest sink simulated by
2 TRENDY-v11 DGVMs is likely due to the lack of detailed processes related to drought-
3 induced mortality and plant hydraulics, such as potential legacy effects from droughts
4 that are not well represented³⁵. It has been estimated that approximately 41% of the
5 whole Amazon forest has been impacted by strong drought events between 2001-
6 2018¹⁹ and one weak, and two moderate to strong drought events happened during
7 our study period (SI Figure 2). Thus, we hypothesise that despite simulating reductions
8 in plant productivity during drought, current estimates from DGVMs are likely
9 underestimating the long-term impact of contemporary drought-induced mortality over
10 Amazon forests. Current studies investigating the fate of the Amazon under climate
11 change using seven Earth System Models from Phase 6 of Coupled Model
12 Intercomparison Project, CMIP6, indicate localised future reductions in vegetation
13 carbon across Amazon by 2100^{55–57}. The inclusion of long-term drought induced tree
14 mortality in current model developments is a priority, and will likely improve Earth
15 System model representation of carbon stocks and fluxes⁵⁸, thus providing a better
16 quantification of the future evolution of the Amazon in response to climate change.

17 Given the large uncertainties from the models used in this research, as well the
18 remaining knowledge gaps on the impacts of forest disturbances on the carbon
19 balance of Amazon, we have insufficient data to confirm whether the whole Amazon
20 was a carbon source, a carbon sink or carbon neutral over the contemporary period
21 according to the bottom-up methods (2010-2020) and the top-down inversion (2010-
22 2018). Our study does however provide further evidence from a range of bottom-up
23 models, as well as top-down inversion that the south-east Amazon was a net land
24 carbon source over the analysed time-period. This result is also corroborated with
25 airborne measurements²⁶. This area of the Amazon has warmed and dried in recent
26 years, particularly during the dry seasons, and it is subject to higher rates of
27 deforestation and fire activity compared to the western Amazon, thus it has increased
28 carbon losses and emissions with compromised forest resilience^{59–61}.

29 Further studies are needed to reconcile the bottom-up and top-down estimates
30 of the net land carbon balance of the Amazon region used in this study. Key areas for
31 future developments are 1) the exploration of how to separate the influence of fluxes
32 from areas surrounding the Amazon due to atmospheric transport of greenhouse
33 gases on the net land carbon fluxes from the top-down inversion; 2) a better
34 representation of drought-induced tree mortality in DGVMs; 3) improved estimates of

1 the impact of forest degradation, including the edge-effect, as well as deforestation on
2 the net land carbon fluxes; 4) improved uncertainty estimations of input data used by
3 bottom-up and top-down models. This could provide a better constraint of
4 local/regional net land fluxes and possibly reconcile estimates based on medium-to-
5 high spatial resolution models, such as the bottom-up approach used in this research.
6 Finally, it is very important to expand and maintain long-term field-inventory
7 measurements, in both old-growth and degraded forests, as well as atmospheric
8 greenhouse gases measurements for model parametrization and quantification of
9 uncertainties.

11 **Conclusion**

12 We provide a state-of-the-art assessment of net land carbon fluxes, the old-
13 growth forest sink, and the anthropogenic forest disturbance for the Amazon using
14 bottom-up and top-down approaches, over 2010-2020. Our analysis shows that we
15 still do not have sufficient data to reconcile bottom-up and top-down estimates of the
16 net carbon balance of Amazon. Spatially, all the model combinations and the top-down
17 inversion suggest that the south-eastern part of the Amazon was a net source of
18 carbon over the analysed period due to deforestation, the impacts of wildfires, and
19 climate trends. This finding agrees with previous studies based on atmospheric
20 greenhouse gases measurements²⁶. Consequently, the south-eastern Amazon acting
21 as net carbon source now may have long-term effects on the Amazon carbon balance,
22 compromising the mitigation potential of the Amazon Forest and the resilience of this
23 ecosystem in a changing climate.

Methods

The key terms in the contemporary net land carbon balance of the Amazon are: i) human disturbance fluxes (i.e., anthropogenic flux) due to land use and land cover changes and degradation, and ii) the old-growth forests sink (i.e., natural sink). In this section, we first present the models used to attribute and estimate the net disturbance fluxes and the net old-growth forest sink over the Brazilian Amazon and Biogeographical Amazon. We then describe the approach used to estimate the net land carbon fluxes with the atmospheric inversion and the combination of the source and sink components from various models.

Disturbance fluxes attribution. We used a set of models to estimate net emissions from different forest disturbance components, such as deforestation, land use and land cover change, and degradation. Note, these disturbance fluxes are reported from different products and can overlap in terms of processes which are defined in Table 2. In this study, we combine different products such that we avoid double-accounting fluxes from the same process. Table 2 includes the main models used to attribute the disturbance fluxes. Further details of each model are given below.

Table 2 Models used to attribute disturbance fluxes for the Brazilian Amazon* and for the whole Biogeographical Amazon[†].

Model	Disturbance area input	Biomass input	Spatial Resolution	Extent	Emissions uncertainty	Gross or net	Main processes	Model reference
*INPE-EM	Based on remote sensing observation; Deforestation areas from PRODES; Degradation areas from DEGRAD and DETER-B;	Spatial; 4th National Inventory of Greenhouse Gases (Brazil MCTI, 2020)	Output 5x5km Input 30mx30m	Brazilian Amazon	NA	Deforestation and degradation gross source and sink flux based on literature response curves (see parameters details in SI Table 1)	Deforestation in old-growth forest only and forest degradation (e.g., forest degradation by fire and logging)	Aguiar et al, 2012; Assis et al, 2020
**BLUE	Based on the Land Use Harmonization 2 (LUH2) dataset. This product uses information on agricultural areas based on the History of the Global Environmental database (HYDE). HYDE is based on in-country FAO statistics and uses the ESA CCI Land Cover maps to scale the in-country areas from FAO to global, spatially explicit estimates. For Brazil it constrains the cropland and grazing areas using MapBiomass c6 areas at the state level. For wood harvest, LUH2 uses FAO/FRA statistics.	Biome level carbon stocks based on literature (Hansis et al, 2015)	0.25°x0.25°	Global	NA	Land use and land use change and forestry gross source and gross sink flux based on carbon densities and response curves from literature (see parameters details in SI Table 2)	Clearing of natural vegetation, including forests, for agricultural expansion (including in shifting cultivation); degradation through logging or use of natural vegetation for rangelands, regrowth of natural vegetation after agricultural abandonment and logging.	Hansis et al, 2015
**GFED	Based on remote sensing observation; Burned area is derived from the Moderate Resolution Imaging Spectroradiometer (MODIS).	Biome level; Modelled by CASA	0.25°x0.25°	Global	1 σ 50% (Global)	Net immediate fire fluxes	Deforestation and degradation fires. GFED considers burned forests are carbon neutral in the long-term. So, GFED presents only immediate emissions and does not account for emissions from late tree mortality due fire occurrence.	van der Werf et al, 2017
**FATE	Based on remote sensing observation; Burned area from MapBiomass fire collection 1 (beta version)	Spatial; Carbon stocks from 4th National Inventory of Greenhouse Gases (Brazil MCTI, 2020)	30mx30m	Brazilian Amazon	NA	Net flux based on field-inventory relationship and scaled-up with remote sensing data (Silva et al, 2020)	Long-term net carbon balance of degradation fires in burned forests not deforested up to 2020. FATE accounts for late tree mortality fluxes due fire occurrence.	Silva et al, in prep

INPE Emission Model (INPE-EM). The INPE-EM is a regional, spatially explicit bookkeeping model to estimate carbon emissions from deforestation based on the bookkeeping model developed by^{62,63} and adapted to the Brazilian Amazon³². INPE-EM accounts for the spatial distribution of biomass stocks and observed deforestation by considering the intra-regional diversity of land use changes practices³².

In this study, we use INPE-EM to provide consolidated estimates of deforestation without degradation (these are accounted for separately) from 2010 to 2020 (available at <http://inpe-em.ccst.inpe.br>) to estimate the annual net deforestation flux for the Brazilian Amazon. The net deforestation estimates from INPE-EM include emissions from clear-cutting of old-growth forests based on official Brazilian deforestation data, called PRODES (Deforestation Monitoring Project in the Legal Amazon by Satellite). It also accounts for the dynamics of regrowth and deforestation of secondary forests and legacy emissions from deforestation in previous years. INPE-EM also provides separate estimates of degradation, which include the trajectories and dynamics of forest degradation (e.g., fire and logging emissions and recovery). The disturbance estimates from INPE-EM used in this study includes the net integrated estimate using deforestation, degradation, and secondary forest fluxes. The degradation input data for INPE-EM is from the satellite-based Brazilian degradation monitoring system²³; we used the DEGRAD product up to 2016 and the DETER-B product thereafter²³. The dynamics of secondary forests implemented in the INPE-EM is based on the land use and land cover maps from the TerraClass product⁶⁴ and the cycles of regrowth and clear-cut of secondary forests from⁶⁵. Details on default parameters used by INPE-EM for each component can be found in SI table 1. Uncertainty estimates are not available for this model because of the difficulties to estimate uncertainty of each input dataset and parameter.

To produce the maps of net fluxes of deforestation and degradation, we used the gridded data from INPE-EM. The original resolution of the INPE-EM spatial output is 5-km and contains the aggregated emission of each grid-cell and comes in a shapefile format. This data was then converted to raster format and re-gridded to 0.5° spatial resolution by aggregating the grid-cells with the sum of fluxes.

Bookkeeping of Land Use Emissions (BLUE). The Bookkeeping of Land Use Emissions (BLUE)³¹ is a spatially explicit global model that tracks carbon emissions and removals due to historical changes and interactions of LULCC in each grid cell.

BLUE follows the bookkeeping approach developed by^{66,67}. BLUE considers the conversion of natural vegetation to agriculture (cropland and pasture) and abandonment^{68,69}. It also includes gross transitions at the sub-grid scale ('shifting cultivation'), transitions between cropland and pasture, and wood harvesting, and accounts for legacy fluxes associated to LULCC over time. The model distinguishes 11 natural plant functional types (PFTs). Average equilibrium biomass densities for the 11 PFTs and cropland and pasture are based on observation-based literature, as are the dynamics of carbon gains or losses, represented via PFT and process-specific response curves, following land-use change and wood harvesting (for the Tropical PFTs see SI Table 2)³¹. Here we use the BLUE simulations that were performed for GCB 2022³⁹.

The land use forcing data used for BLUE in GCB 2022 and thus in our study is the gridded LUH2 data set^{68,69} (GCB 2022 version), which provides historical sub-grid-scale transitions between land-use and land-cover categories, such as primary and secondary natural land, cropland, pasture, rangeland, and urban land^{68,69}. LUH2 incorporates multiple datasets at different spatial and temporal scales to produce a global gridded land use dataset. For example, it uses inputs from the History Database of the Global Environment (HYDE 3.3)⁷⁰ for cropland and grazing areas, which are derived from FAO (Food Agriculture Organization) national statistical data (and sub-national where available) and spatially allocated based on the ESA Climate Change Initiative (ESA CCI) land cover annual maps^{68,69}. Therefore, the LUH2 natural vegetation cover is not constrained directly by observations, such as remote sensing data. Recently, there has been a major update in the LUH2/HYDE 3.3 (GCB 2021 version) in cropland and pasture areas for Brazil derived from Food and Agriculture Organization (FAO) national statistics due to double-cropping issues⁷¹, and the adoption of multi-year ESA CCI land cover maps. This update improved the spatial allocation of land use changes within Brazil, but it still underestimated the fluxes estimates when based directly from remote sensing products such as the MapBiomas LULCC maps³⁶. Furthermore, there is latency in FAO statistics, and annual data until 2017 was used in HYDE3.3. To extrapolate to the end of 2021, a trend from the last five years of data (2012-17) is typically applied, which does not capture the recent upturn in deforestation for Brazil¹³. To better represent and improve the magnitude of LULCC in Brazil and consequently in the Amazon, the cropland and grazing areas of LUH2/HYDE3.3 (GCB 2022 version) dataset for the years 1700-2021 used by BLUE³⁹

1 was based on the areas derived from the remote sensing classification from
2 MapBiomass (collection 6) maps at state level for the contemporary period (1985 until
3 year 2020), and then spatially allocated by the HYDE 3.3 algorithm. Due to challenges
4 of estimating uncertainties of input parameters from the BLUE model, there is currently
5 no regional uncertainty estimate available.

6 In this study we provide estimates of the net land use and land cover change
7 emissions (E_{LUC}) for both study regions (Brazilian Amazon and Biogeographical
8 Amazon) from the global BLUE model. To produce the E_{LUC} maps, BLUE output at
9 0.25° spatial resolution was converted to raster format and re-gridded to 0.5° of spatial
10 resolution with the aggregated sum of the fluxes.

11 **FATE forest degradation fire flux estimate.** The fire bookkeeping model (FATE) is
12 a spatiotemporal model to estimate long-term net emissions from Amazon Forest fires.
13 This is a spatially explicit approach based on²¹ which has been developed in
14 partnership with the Brazilian Greenhouse Gas Emission and Removal Estimating
15 System (SEEG) project and FATE network. The model is parametrized with a dataset
16 derived from field information of burned plots in the Amazon and includes estimates
17 of combustion emissions, as well as post-fire temporal biomass changes and delayed
18 mortality and recovery²¹. The model is scaled-up to the Brazilian Amazon using the
19 time-series of burned area (MapBiomass fire collection 1)⁵³ and the biomass map
20 derived from the 4th National Communication of the National Inventory of greenhouse
21 gases (MCTIC,2020).

22 This burned area product is based on a time-series of Landsat mosaics for the
23 entire Brazil with spatial resolution of 30mx30m over the period 1985-2020. To classify
24 the burned pixels, MapBiomass fire uses a deep learning algorithm (Deep Neural
25 Network) within the Google Earth Engine platform. The methodology also takes
26 advantage of ancillary data, such as the burned area product MC64A1 and the fire
27 hotspot data from INPE to train the algorithm. The reported average accuracy of
28 burned areas from MapBiomass fire was 89.35%⁵³. However, it presents a conservative
29 estimate (i.e., an underestimate) due to the limitations associated with the temporal
30 availability of Landsat images, mainly in areas with high cloud coverage, such as the
31 Amazon and the difficulty to map low intensity understory fires⁵³.

32 To estimate only the emissions from degraded forests by fire, the burned area
33 product was overlaid with the deforestation data and LULCC maps from MapBiomass

to exclude the pixels that were deforested (e.g., deforestation fires) and fires outside forest pixels. The biomass product from the 4th National Inventory of Greenhouse Gases⁷² was used to estimate the biomass stocks and necromass. The mortality parameters were based on a previous study²¹ and additional permanent plots with measurements before and after fires, and the combustion loss and decomposition parameters were derived from literature. Formal uncertainty is not provided due to difficulties in propagating the uncertainty of the input data. The spatial output is available at a 30mx30m spatial resolution with the net CO₂ flux over 1985-2020. To convert to carbon, we multiplied the values by the conversion factor CO₂ - C of 12/44. We then summed the values within the Brazilian Amazon limits to produce the total annual data. To produce the spatial maps of net CO₂ flux of burned forests from forest degradation by fire in the Brazilian Amazon, we aggregated it to 0.5° spatial resolution using the sum of the grid-cells to facilitate the comparison with the global models at a coarse spatial resolution. In this study, we add the FATE forest degradation flux from the Brazilian Amazon to E_{LUC} from BLUE (which lacks degradation from fires) to provide an integrated estimate of the total disturbance from land use and land cover changes emissions and degradation.

Global Fire Emissions Database (GFED). As an additional estimate of the disturbance emissions from deforestation and degradation for both the Brazilian Amazon and the whole Biogeographical Amazon, we used the Global Fire Emissions Database (GFED4.1s). The GFED is a modelling system based on the Carnegie-Ames-Stanford Approach (CASA) biogeochemical model and has a spatial resolution of 0.25°x0.25°⁴⁰. The burned area input of GFED is derived from MODIS (MCD64A1 product)⁴⁶, which provide daily burned area at 500m spatial resolution and then GFED aggregates to a 0.25° grid. Formal uncertainty is not provided by GFED due to difficulties in assessing uncertainty of various layers used in the modelling. However, the best-guess global uncertainty provided could be 1σ 50%⁴⁰. In our analysis we extracted and aggregated the GFED annual emissions associated with tropical forest fires, which include burned biomass due to both deforestation and degradation processes, within both the Brazilian Amazon and the whole Biogeographical Amazon limits. Then, the spatial GFED maps were aggregated to 0.5° spatial resolution using the sum of the grid-cell fluxes.

Old-growth Forest carbon sink estimates. The old-growth forest sink was estimated from a multi-model mean of 16 DGVMs from the Trends in the land carbon cycle project (TRENDY-v11), using the simulations performed for GCB 2022³⁹. Each DGVM performed factorial simulations for TRENDY-v11 to attribute the carbon exchange to individual environmental drivers. To estimate the old-growth forest sink we used TRENDY-v11 simulation 2 (S2) which uses time varying atmospheric CO₂ concentrations, nitrogen deposition, and climate with a time-invariant pre-industrial (year 1700) land cover distribution. This approach is used by the Global Carbon Budget assessments to calculate the natural terrestrial sink. More details about the DGVM processes relevant for the intact sink can be found in SI Table 3. S2 does not account for LULCC dynamics, and thus includes the impact of environmental changes on land that in reality has been modified by humans. This leads to a large CO₂ induced carbon sink in forests that existed in 1700, but do not exist anymore today. Previous work estimated this additional carbon flux to be ~100 Tg C yr⁻¹ for Brazil over 2000-2020⁷³. To mask out the proportion of the old-growth sink within disturbed grid-cells and account only for the sink from old-growth forests, we used a mask from INPE based on the Brazilian Amazon official annual accumulated deforestation data available since 1988 and for degradation data since 2007 (SI Figure 5). To maintain consistency in the old-growth forest mask, we used only the official data provided from INPE since it has a better manual control of its forest mask over time compared to other remote sensing-based products that rely on automatic classification and just account for degradation in primary forest pixels. However, this data is available only for Brazil and the degradation estimates start in 2007; consequently, it constitutes a conservative estimate of the old-growth forest fraction. Therefore, the old-growth sink estimates obtained with this mask could potentially still overestimate part of the natural sink in the non-Brazilian Amazon countries (i.e., western and north region). The application of this mask reduced the whole Amazon natural sink simulated by TRENDY-V11 models from -362 (± 220 1SD) Tg C yr⁻¹ to -333 (± 195) Tg C yr⁻¹ over 2010-2020 (SI Figure 8). We applied this mask to each DGVM from TRENDY-V11. Then the annual old-growth sink was extracted for each model within the limits of both the Biogeographical Amazon shapefile and the Brazilian Amazon biome. Finally, we calculated the multi-model mean and standard deviation statistics. To evaluate the correlation between the annual variation of the old-growth forest sink and the drought

effects from ENSO years, we used as a drought metric the Annual Maximum Cumulative Water Deficit⁴³ (MCWD) based on the precipitation data from CRUJRA2.4^{74–76}. The MCWD is an indicator of meteorologically induced water stress in forests. We then extracted the average annual MCWD within the Brazilian Amazon and Biogeographical Amazon domains and performed a correlation analysis (Pearson’s correlation test) between the annual old-growth forest sink and the MCWD. In order to assess the old-growth sink simulated by the DGVMs, we compared it against RAINFOR inventory based estimates^{8,9,44} for the common period (2010-2015) by using a Welch’s t-test to test whether the averages over the same period were significantly different. Additionally, we did a similar test comparing the aboveground carbon changes (AGC) in old-growth forests based on L-VOD¹² and the AGC changes based on the TRENDY-v11 multi-model mean between 2011 and 2019. We used the annual biomass data from each model of TRENDY-v11 to calculate the change between the years and compare to AGC based on L-VOD. Since the biomass variable from TRENDY-v11 accounts also for belowground biomass, we assumed that 20% of this biomass is belowground based on previous studies⁷⁷ and applied a factor of 0.8 to each grid-cell to extract the aboveground stock. Finally, we performed a Welch’s t-test to test whether the averages over the same period were significantly different.

Net land flux approaches. To quantify the net carbon exchange flux between land and atmosphere we used the chemical transport model TOMCAT⁷⁸ and its inverse model, INVICAT⁷⁹. The data was produced using a variational (4D-var) inverse model to optimise monthly non-fossil fuel land and ocean carbon fluxes through assimilation of in situ flask data from the Global Monitoring Laboratory (GML) of the National Oceanic and Atmospheric Administration (NOAA)⁸⁰. A new addition to this model was the use of independent in situ lower-troposphere observations by aircraft-borne flask of greenhouse gases (CO₂) made within the Amazon basin since 2010⁴⁹, thus providing a better-constrained regional estimate. The a priori inversion input was based on the Carnegie-Ames-Stanford model (CASA) for land fluxes. A climatology was used as a prior for the CASA fluxes, so all posterior variation was provided by the atmospheric observation data and varying meteorology. In addition to the CASA land fluxes as prior, TOMCAT inputs include fossil fuel data from the Carbon Dioxide Information Analysis Center (CDIAC) and ocean flux was a combination of gridded estimates^{81,82}, as in previous TOMCAT inversions⁸⁰ scaled to the Global Carbon

Project (GCP) values. Prior emissions are given grid cell uncertainties of 308% of the prior flux value. Also, for the assimilated observation data from both surface monitoring sites and the vertical profile sites⁸³ uncorrelated random errors of 1 ppm were attributed to each observation. The TOMCAT output is available as monthly estimates between 2010 and 2018 with a 5.6°x5.6° spatial resolution³⁸. In our analysis we calculated the annual mean of each grid cell for each year and then the total fluxes within the Brazilian Amazon and Biogeographical Amazon limits.

To calculate a 'bottom-up' approach of the net carbon flux, we first combined the net source (deforestation + degradation) and net natural sink in old-growth forests from TRENDY-v11 S2 simulation, which is similar to the Global Carbon Budget annual assessments methodology. As the net source term (+) for the Brazilian Amazon, we used a multi-model average of the regional bookkeeping model (INPE-EM with degradation), the global bookkeeping model (BLUE) with the net forest degradation flux from FATE added, as well as deforestation and degradation fire emissions from GFED (Table 3). For the Biogeographical Amazon, due to data availability limitations, the disturbance term was based separately on bottom-up and hybrid approaches (see Table 3). A summary of the main input and processes within each of the disturbance models can be found in Table 2. The old-growth forest sink term (-) was calculated using the annual multi-model average from TRENDY-v11 DGVMs over 2010-2020. To calculate the uncertainty of the net land carbon fluxes from the 'bottom-up' approach, we propagated the uncertainty by using the annual standard deviation of the average disturbance estimate and old-growth forest sink based on DGVMs. Since the bottom-up disturbance models differ in their spatial extent (e.g., Brazilian Amazon and Biogeographical Amazon), we used a different combination for each region (Table 3). Spatial model outputs also differ in their spatial resolution and to avoid further error inclusion from spatial resampling, the annual values for the Brazilian Amazon and Biogeographical Amazon were extracted using each model's original spatial resolution. Then, to produce the net carbon flux maps we spatially resampled the bottom-up approaches to a standard spatial resolution of 0.5° x 0.5°.

For the whole biogeographical Amazon, we provide an additional estimate of the net land carbon fluxes from the CARbon Data Model fraMework (CARDAMOM)^{41,42}. CARDAMOM uses a Bayesian approach within an Adaptive Proposal – Markov Chain Monte Carlo (AP-MCMC)⁸⁴ to retrieve parameters, at pixel scale, for the

intermediate complexity C-cycle model DALEC⁸⁵. Observational constraints include earth observation datasets and databased information on soil C stocks. Fire is imposed based on the MODIS Burned area product (MCD64A1) while deforestation was imposed based on the Global Forest Watch Forest loss estimates. The atmospheric CO₂ driving dataset was based on the input for the TRENDY-v11 protocol from GCB 2022³⁹. The climate driving data was based on Climatic Research Unit gridded Time Series (CRU-TS 4.06)⁷⁴ and Climatic Research Unit and Japanese reanalysis data (CRU-JRA v2.4). In this work we used the CARDAMOM version compatible to TRENDY-v11 protocol and the net land carbon fluxes was based on the net biome productivity output from simulation 3 (S3), which accounts for changes in atmospheric CO₂ concentration, climate and land use over time. The output is available as annual estimates over 2000 and 2021 in a global grid of 1°x1° spatial resolution. Spatial uncertainty estimates were provided by CARDAMOM including explicit propagation of ensemble uncertainty from monthly to annual time scales. The annual net land carbon fluxes and its uncertainty from CARDAMOM were calculated within the limits of the whole biogeographical Amazon region over 2010 and 2020.

Table 3 Components used to calculate the net land carbon flux for the Brazilian Amazon and the whole Biogeographical Amazon. Details of each component of the disturbance models are given in Table 2.

Name	Brazilian Amazon	Biogeographical Amazon
	Net disturbance (+):	Net disturbance (+):
	Multi-model average of INPE-EM (deforestation + degradation); BLUE E _{LUC} + FATE net degradation fire flux; GFED (net deforestation and degradation)**	BLUE E _{LUC} + FATE net degradation fire flux*
Bottom-up	Net old-growth forest sink (-): TRENDY-v11 Multi-model average ³⁹	Net old-growth forest sink (-): TRENDY-v11 Multi-model average ³⁹
	The bottom-up net land flux is calculated from the sum of the net disturbance multi-model average and the TRENDY-v11 net old-growth forest sink	The bottom-up net land flux is calculated from the sum of net disturbance flux of BLUE+FATE and TRENDY-v11 net old-growth forest sink

<hr/>		
		Disturbance (+): GFED (net deforestation and degradation)**
Hybrid	-	Net old-growth forest sink (-): TRENDY-v11 Multi-model average ³⁹
The hybrid net land flux is calculated from the sum of GFED net fire emissions and TRENDY-v11 net old-growth forest sink		
CARDAMOM	-	Net land flux from CARDAMOM model^{41,42}
<hr/>		
Top-down inversion	Net land flux from TOMCAT atmospheric inversion³⁸	Net land flux from TOMCAT atmospheric inversion³⁸

* Note that the FATE net wildfire flux is available only for the Brazilian Amazon, thus we potentially underestimate this flux for the whole Biogeographical Amazon. ** Note that GFED net estimates considers degraded forests by fire as carbon neutral; whereas FATE includes late tree mortality fluxes.

Data availability

INPE-EM deforestation and degradation estimates are freely available at <http://inpe-em.ccst.inpe.br/emissoes-liquidadas-com-degracao-amz/>. FATE dataset upon reasonable request to Camila Silva. The atmospheric inversion spatial data is available upon reasonable request to Luana S. Basso. The independent in situ lower-troposphere observations by aircraft-borne flask of greenhouse gases (CO₂) made within the Amazon basin since 2010 by Luciana Gatti group and used in the atmospheric inversion are available from PANGAEA Data Archiving at <https://doi.org/10.1594/PANGAEA.926834> for data from 2010 to 2018 and at <https://doi.pangaea.de/10.1594/PANGAEA.949643> for 2019 and 2020. GFED4 fire emissions is freely available at <https://www.globalfiredata.org/>. TRENDYv11 DGVMs used in the Global Carbon Budget 2022 and in this research can be requested at <https://globalcarbonbudgetdata.org/closed-access-requests.html>. BLUE land use and land use change emissions is available upon reasonable request to Julia Pongratz

and Clemens Schwingshackl. CARDAMOM dataset is available upon reasonable request to Luke Smallman. The annual carbon fluxes from each model used in this research (disturbances, old-growth sink and net flux) for the Brazilian Amazon and whole Biogeographical Amazon are available in the Supplementary excel tables 4 and 5, respectively.

Code availability

The code and tables used to reproduce the main paper graphics of Figures 2a,b, 3a,b, 4a and 5a are available in Zenodo doi:10.5281/zenodo.8348435 (this link will be available upon publication). Further editions to combine the layout of graphics and maps were made in a design software (InkScape).

Acknowledgements

The development of this research has been supported by the Newton Fund through the Met Office Climate Science for Service Partnership Brazil (CSSP Brazil), RECCAP2 project which is part of the ESA Climate Change Initiative (contract no. 4000123002/18/I-NB), and the H2020 European Institute of Innovation and Technology (4C; Grant No. 821003). C.W. is funded via UK National Centre for Earth Observation (NE/R016518/1 and NE/N018079/1). L.S.B is funded by State of Sao Paulo Science Foundation - FAPESP (2018/14006-4, 2020/02656-4). L.G. was funded by CARBAM project (FAPESP 2016/02018-2). ORNL is managed by UT-Battelle, LLC, for the DOE under contract DE-AC05-1008 00OR22725. For the purpose of open access, the author has applied a 'Creative Commons Attribution (CC BY) licence to any Author Accepted Manuscript version arising. We thank Ian Harris for advising us on the CRUJRA forcing dataset.

Contributions

TMR, SS, EG and LEOCA designed the study. TMR, MOS, LSB, CW, CS compiled the data. TMR conducted the data analysis. TMR and SS led the writing of the manuscript to which all authors contributed with inputs. JP and CIS provided the BLUE bookkeeping model. AA, VKA, SF, AKJ, EK, DK, JK, MOS, BP, QS, HT, APW, WY, XY, and SZ provided the dynamic global vegetation models, with synthesis by TMR and MOS. LSB, CW and EG provided the atmospheric inversion. CS provided the net

fluxes of fire degradation (FATE) in the Brazilian Amazon. FGSB and CvR provided the INPE-EM data. MW and LS provided the CARDAMOM net biome productivity data.

References

1. Malhi, Y. *et al.* The regional variation of aboveground live biomass in old-growth Amazonian forests. *Global Change Biology* **12**, 1107–1138 (2006).
2. Gloor, M. *et al.* The carbon balance of South America: A review of the status, decadal trends and main determinants. *Biogeosciences* **9**, 5407–5430 (2012).
3. Feldpausch, T. R. *et al.* Tree height integrated into pantropical forest biomass estimates. *Biogeosciences* **9**, 3381–3403 (2012).
4. Albert, J. S. *et al.* Human impacts outpace natural processes in the Amazon. *Science* **379**, eabo5003 (2023).
5. Lawrence, D. & Vandecar, K. Effects of tropical deforestation on climate and agriculture. *Nature Clim Change* **5**, 27–36 (2015).
6. Nobre, C. A. *et al.* Land-use and climate change risks in the Amazon and the need of a novel sustainable development paradigm. *Proceedings of the National Academy of Sciences* **113**, 10759–10768 (2016).
7. Leite-Filho, A. T., Soares-Filho, B. S., Davis, J. L., Abrahão, G. M. & Börner, J. Deforestation reduces rainfall and agricultural revenues in the Brazilian Amazon. *Nature Communications* **12**, 1–7 (2021).
8. Hubau, W. *et al.* Asynchronous carbon sink saturation in African and Amazonian tropical forests. *Nature* **579**, 80–87 (2020).
9. Brienen, R. J. W. *et al.* Long-term decline of the Amazon carbon sink. *Nature* **519**, 344–348 (2015).

10. Doughty, C. E. *et al.* Drought impact on forest carbon dynamics and fluxes in Amazonia. *Nature* **519**, 78–82 (2015).
11. Doughty, C. E. *et al.* Tropical forests are approaching critical temperature thresholds. *Nature* 1–7 (2023) doi:10.1038/s41586-023-06391-z.
12. Fawcett, D. *et al.* Declining Amazon biomass due to deforestation and subsequent degradation losses exceeding gains. *Global Change Biology* **n/a**, (2022).
13. Silva Junior, C. H. L. *et al.* The Brazilian Amazon deforestation rate in 2020 is the greatest of the decade. *Nature Ecology and Evolution* **5**, 144–145 (2021).
14. Kruid, S. *et al.* Beyond Deforestation: Carbon Emissions From Land Grabbing and Forest Degradation in the Brazilian Amazon. *Frontiers in Forests and Global Change* **4**, (2021).
15. Qin, Y. *et al.* Carbon loss from forest degradation exceeds that from deforestation in the Brazilian Amazon. *Nature Climate Change* **11**, 442–448 (2021).
16. Matricardi, E. A. T. *et al.* Long-term forest degradation surpasses deforestation in the Brazilian Amazon. *Science* **369**, 1378–1382 (2020).
17. Aragão, L. E. O. C. *et al.* 21st Century drought-related fires counteract the decline of Amazon deforestation carbon emissions. *Nature Communications* **9**, 1–12 (2018).
18. Bullock, E. L., Woodcock, C. E., Souza, C. & Olofsson, P. Satellite-based estimates reveal widespread forest degradation in the Amazon. *Global Change Biology* **26**, 2956–2969 (2020).
19. Lapola, D. M. *et al.* The drivers and impacts of Amazon forest degradation. *Science* **379**, eabp8622 (2023).
20. Heinrich, V. H. A. *et al.* Large carbon sink potential of secondary forests in the Brazilian Amazon to mitigate climate change. *Nature Communications* **12**, 1–11 (2021).

- 1 21. Silva, C. V. J. *et al.* Estimating the multi-decadal carbon deficit of burned Amazonian
2 forests. *Environmental Research Letters* **15**, (2020).
- 3 22. Silva Junior, C. H. L. *et al.* Persistent collapse of biomass in Amazonian forest edges
4 following deforestation leads to unaccounted carbon losses. *Science Advances* **6**,
5 eaaz8360 (2020).
- 6 23. Assis, T. O. *et al.* CO₂ emissions from forest degradation in Brazilian Amazon.
7 *Environmental Research Letters* **15**, 104035 (2020).
- 8 24. Harris, N. L. *et al.* Global maps of twenty-first century forest carbon fluxes. *Nature*
9 *Climate Change* **11**, 234–240 (2021).
- 10 25. Tejada, G. *et al.* CO₂ emissions in the Amazon: are bottom-up estimates from land use
11 and cover datasets consistent with top-down estimates based on atmospheric
12 measurements? *Frontiers in Forests and Global Change* **6**, (2023).
- 13 26. Gatti, L. V. *et al.* Amazonia as a carbon source linked to deforestation and climate
14 change. *Nature* **595**, 388–393 (2021).
- 15 27. Aragão, L. E. O. C. *et al.* Environmental change and the carbon balance of Amazonian
16 forests. *Biological Reviews* **89**, 913–931 (2014).
- 17 28. Hansen, M. C. *et al.* High-Resolution Global Maps of 21st-Century Forest Cover Change.
18 *Science* **342**, 850–853 (2013).
- 19 29. Sitch, S. *et al.* Recent trends and drivers of regional sources and sinks of carbon dioxide.
20 *Biogeosciences* **12**, 653–679 (2015).
- 21 30. Houghton, R. A. & Nassikas, A. A. Global and regional fluxes of carbon from land use and
22 land cover change 1850–2015. *Global Biogeochemical Cycles* **31**, 456–472 (2017).
- 23 31. Hansis, E., Davis, S. J. & Pongratz, J. Relevance of methodological choices for accounting
24 of land use change carbon fluxes. *Global Biogeochemical Cycles* **29**, 1230–1246 (2015).

32. Aguiar, A. P. D. *et al.* Modeling the spatial and temporal heterogeneity of deforestation-driven carbon emissions: The INPE-EM framework applied to the Brazilian Amazon. *Global Change Biology* **18**, 3346–3366 (2012).
33. Peylin, P. *et al.* Global atmospheric carbon budget: results from an ensemble of atmospheric CO₂ inversions. <https://bg.copernicus.org/preprints/10/5301/2013/bgd-10-5301-2013.pdf> (2013) doi:10.5194/bgd-10-5301-2013.
34. Kondo, M. *et al.* State of the science in reconciling top-down and bottom-up approaches for terrestrial CO₂ budget. *Global Change Biology* **26**, 1068–1084 (2020).
35. McDowell, N. *et al.* Drivers and mechanisms of tree mortality in moist tropical forests. *New Phytologist* **219**, 851–869 (2018).
36. Rosan, T. M. *et al.* A multi-data assessment of land use and land cover emissions from Brazil during 2000–2019. *Environmental Research Letters* **16**, 074004 (2021).
37. Albert, J. *et al.* The multiple viewpoints for the Amazon: geographic limits and meanings. https://www.theamazonwewant.org/wp-content/uploads/2021/09/220105_The-multiple-viewpoints-for-the-Amazon-formatted-and-reviewed-050122.pdf (2021).
38. Basso, L. S. *et al.* Atmospheric CO₂ inversion reveals the Amazon as a minor carbon source caused by fire emissions, with forest uptake offsetting about half of these emissions. *Atmospheric Chemistry and Physics* **23**, 9685–9723 (2023).
39. Friedlingstein, P. *et al.* Global Carbon Budget 2022. *Earth System Science Data* **14**, 4811–4900 (2022).
40. Van Der Werf, G. R. *et al.* Global fire emissions estimates during 1997–2016. *Earth System Science Data* **9**, 697–720 (2017).

- 1 41. Bloom, A. A. & Williams, M. Constraining ecosystem carbon dynamics in a data-limited
2 world: integrating ecological ‘common sense’ in a model–data fusion framework.
3 *Biogeosciences* **12**, 1299–1315 (2015).
- 4 42. Bloom, A. A., Exbrayat, J.-F., van der Velde, I. R., Feng, L. & Williams, M. The decadal
5 state of the terrestrial carbon cycle: Global retrievals of terrestrial carbon allocation,
6 pools, and residence times. *Proceedings of the National Academy of Sciences* **113**, 1285–
7 1290 (2016).
- 8 43. Aragão, L. E. O. C. *et al.* Spatial patterns and fire response of recent Amazonian
9 droughts. *Geophysical Research Letters* **34**, (2007).
- 10 44. Phillips, O. L. *et al.* Carbon uptake by mature Amazon forests has mitigated Amazon
11 nations’ carbon emissions. *Carbon Balance and Management* **12**, 1–9 (2017).
- 12 45. INPE. Emissões líquidas com degradação. *Inpe-EM* [http://inpe-](http://inpe-em.ccst.inpe.br/emissoes-liquidadas-com-degracao-amz/)
13 [em.ccst.inpe.br/emissoes-liquidadas-com-degracao-amz/](http://inpe-em.ccst.inpe.br/emissoes-liquidadas-com-degracao-amz/).
- 14 46. Giglio, L., Boschetti, L., Roy, D. P., Humber, M. L. & Justice, C. O. The Collection 6 MODIS
15 burned area mapping algorithm and product. *Remote Sensing of Environment* **217**, 72–
16 85 (2018).
- 17 47. Aragão, L. E. O. C. *et al.* 21st Century drought-related fires counteract the decline of
18 Amazon deforestation carbon emissions. *Nature Communications* **9**, 1–12 (2018).
- 19 48. Barlow, J., Berenguer, E., Carmenta, R. & França, F. Clarifying Amazonia’s burning crisis.
20 *Global Change Biology* **26**, 319–321 (2020).
- 21 49. Gatti, L. V. *et al.* Increased Amazon carbon emissions mainly from decline in law
22 enforcement. *Nature* 1–6 (2023) doi:10.1038/s41586-023-06390-0.

50. Trancoso, R. Changing Amazon deforestation patterns: Urgent need to restore command and control policies and market interventions. *Environmental Research Letters* **16**, (2021).
51. West, T. A. P. & Fearnside, P. M. Brazil's conservation reform and the reduction of deforestation in Amazonia. *Land Use Policy* **100**, 105072 (2021).
52. Friedlingstein, P. *et al.* Global Carbon Budget 2021. 1917–2005 (2022).
53. Alencar, A. A. C. *et al.* Long-Term Landsat-Based Monthly Burned Area Dataset for the Brazilian Biomes Using Deep Learning. *Remote Sensing* **14**, 2510 (2022).
54. O'Sullivan, M. *et al.* Process-oriented analysis of dominant sources of uncertainty in the land carbon sink. *Nat Commun* **13**, 4781 (2022).
55. Parry, I. M., Ritchie, P. D. L. & Cox, P. M. Evidence of localised Amazon rainforest dieback in CMIP6 models. *Earth System Dynamics* **13**, 1667–1675 (2022).
56. Ritchie, P. D. L., Parry, I., Clarke, J. J., Huntingford, C. & Cox, P. M. Increases in the temperature seasonal cycle indicate long-term drying trends in Amazonia. *Commun Earth Environ* **3**, 1–8 (2022).
57. Parsons, L. A. Implications of CMIP6 Projected Drying Trends for 21st Century Amazonian Drought Risk. *Earth's Future* **8**, e2020EF001608 (2020).
58. Anderegg, W. R. L. & Venturas, M. D. Plant hydraulics play a critical role in Earth system fluxes. *New Phytologist* **226**, 1535–1538 (2020).
59. Staal, A. *et al.* Feedback between drought and deforestation in the Amazon. *Environmental Research Letters* **15**, (2020).
60. Barkhordarian, A., Saatchi, S. S., Behrangi, A., Loikith, P. C. & Mechoso, C. R. A Recent Systematic Increase in Vapor Pressure Deficit over Tropical South America. *Scientific Reports* **9**, 1–12 (2019).

61. Boulton, C. A., Lenton, T. M. & Boers, N. Pronounced loss of Amazon rainforest resilience since the early 2000s. *Nature Climate Change* **12**, (2022).
62. Houghton, R. A. Why are estimates of the terrestrial carbon baance so different? *Global Change Biology* **9**, 500–509 (2003).
63. Houghton, R. a *et al.* Annual fluxes of carbon from deforestation and regrowth in the Brazilian Amazon. *Nature* **403**, 301–304 (2000).
64. ALMEIDA, C. A. de *et al.* High spatial resolution land use and land cover mapping of the Brazilian Legal Amazon in 2008 using Landsat-5/TM and MODIS data. *Acta Amazonica* **46**, 291–302 (2016).
65. Almeida, C. A. Estimativa da área e do tempo de permanência da vegetação secundária na Amazônia Legal por meio de imagens Landsat/TM. *Sensoriamento Remoto Mestrado*, 130 (2009).
66. Houghton, R. A. Revised estimates of the annual net flux of carbon to the atmosphere from changes in land use and land management 1850-2000. *Tellus, Series B: Chemical and Physical Meteorology* **55**, 378–390 (2003).
67. Houghton, R. A. *et al.* Annual fluxes of carbon from deforestation and regrowth in the Brazilian Amazon. *Nature* **403**, 301–304 (2000).
68. Chini, L. *et al.* Land-use harmonization datasets for annual global carbon budgets. *Earth System Science Data* **13**, 4175–4189 (2021).
69. Hurtt, G. *et al.* Harmonization of Global Land-Use Change and Management for the Period 850–2100 (LUH2) for CMIP6. *Geoscientific Model Development Discussions* 1–65 (2020) doi:10.5194/gmd-2019-360.
70. Goldewijk, K. K., Beusen, A., Doelman, J. & Stehfest, E. Anthropogenic land use estimates for the Holocene - HYDE 3.2. *Earth System Science Data* **9**, 927–953 (2017).

- 1 71. Novaes, R. M. L. *et al.* Brazil ' s agricultural land , cropping statistics and new estimates.
2 (2022).
- 3 72. Brazil MCTI. FOURTH NATIONAL COMMUNICATION OF BRAZIL TO THE UNITED NATIONS
4 FRAMEWORK CONVENTION ON CLIMATE CHANGE. (2020).
- 5 73. Obermeier, W. A. *et al.* Modelled land use and land cover change emissions-a spatio-
6 Temporal comparison of different approaches. *Earth System Dynamics* **12**, 635–670
7 (2021).
- 8 74. Harris, I., Osborn, T. J., Jones, P. & Lister, D. Version 4 of the CRU TS monthly high-
9 resolution gridded multivariate climate dataset. *Sci Data* **7**, 109 (2020).
- 10 75. Harris, I., Jones, P. D., Osborn, T. J. & Lister, D. H. Updated high-resolution grids of
11 monthly climatic observations - the CRU TS3.10 Dataset. *International Journal of*
12 *Climatology* **34**, 623–642 (2014).
- 13 76. KOBAYASHI, S. *et al.* The JRA-55 Reanalysis: General Specifications and Basic
14 Characteristics. *Journal of the Meteorological Society of Japan. Ser. II* **93**, 5–48 (2015).
- 15 77. Gibbs, H. K., Brown, S., Niles, J. O. & Foley, J. A. Monitoring and estimating tropical
16 forest carbon stocks: making REDD a reality. *Environ. Res. Lett.* **2**, 045023 (2007).
- 17 78. Chipperfield, M. P. New version of the TOMCAT/SLIMCAT off-line chemical transport
18 model: Intercomparison of stratospheric tracer experiments. *Quarterly Journal of the*
19 *Royal Meteorological Society* **132**, 1179–1203 (2006).
- 20 79. Wilson, C., Chipperfield, M. P., Gloor, M. & Chevallier, F. Development of a variational
21 flux inversion system (INVICAT v1.0) using the TOMCAT chemical transport model.
22 *Geoscientific Model Development* **7**, 2485–2500 (2014).

- 1 80. Gloor, E. *et al.* Tropical land carbon cycle responses to 2015/16 El Niño as recorded by
2 atmospheric greenhouse gas and remote sensing data. *Philosophical Transactions of the*
3 *Royal Society B: Biological Sciences* **373**, 20170302 (2018).
- 4 81. Takahashi, T. *et al.* Climatological mean and decadal change in surface ocean pCO₂, and
5 net sea–air CO₂ flux over the global oceans. *Deep Sea Research Part II: Topical Studies in*
6 *Oceanography* **56**, 554–577 (2009).
- 7 82. Khatiwala, S., Primeau, F. & Hall, T. Reconstruction of the history of anthropogenic CO₂
8 concentrations in the ocean. *Nature* **462**, 346–349 (2009).
- 9 83. Gatti, L. V. *et al.* Drought sensitivity of Amazonian carbon balance revealed by
10 atmospheric measurements. *Nature* **506**, 76–80 (2014).
- 11 84. Haario, H., Saksman, E. & Tamminen, J. An adaptive Metropolis algorithm. *Bernoulli* **7**,
12 223–242 (2001).
- 13 85. Williams, M., Schwarz, P. A., Law, B. E., Irvine, J. & Kurpius, M. R. An improved analysis
14 of forest carbon dynamics using data assimilation. *Global Change Biology* **11**, 89–105
15 (2005).
- 16
17
18
19